HHS Public Access

Author manuscript

JAMA Ophthalmol. Author manuscript; available in PMC 2020 February 01.

Published in final edited form as:

JAMA Ophthalmol. 2019 February 01; 137(2): 176–183. doi:10.1001/jamaophthalmol.2018.5654.

Examination of Coats' Disease in a Pediatric Population Using Optical Coherence Tomography, Fundus Photos, Fluorescein Angiography, and Histopathologic Analysis

Sally S. Ong, MD[1,2], **Thomas J. Cummings, MD**[3], **Lejla Vajzovic, MD**[2], **Prithvi Mruthyunjaya, MD, MHS**[4], **Cynthia A. Toth, MD**[2]

[1]Department of Ophthalmology, Wilmer Eye Institute, Johns Hopkins University School of Medicine, Baltimore, Maryland [2]Department of Ophthalmology, Duke University Medical Center, Durham, North Carolina [3]Department of Pathology, Duke University Medical Center, Durham, North Carolina [4]Department of Ophthalmology, Stanford University Medical Center, Palo Alto, California

Abstract

Importance: Coats' disease is a rare pediatric vitreoretinopathy but can cause devastating visual and anatomic outcomes.

Objective: To compare optical coherence tomography (OCT) to fundus photos (FP), fluorescein angiography (FA) and histopathologic findings in Coats' disease.

Design: Retrospective cohort study.

Setting: Single tertiary institution

Participants: Twenty-eight children with Coats' disease were identified through a review of medical charts from December 2002 to January 2018. Four eyes were obtained from a biorepository for histopathologic analysis.

Main Outcomes and Measures: Macular OCT, FP and FA were reviewed and compared for morphological changes. These were compared to retinal histopathological findings.

Corresponding author: Cynthia A. Toth, MD, Department of Ophthalmology, Duke University, Eye Center, 2351 Erwin Road, Durham, NC 27710, Phone: 919-684-5631, Fax: 919-681-6474, cynthia.toth@duke.edu.

Author Contributions:

Dr Toth had full access to all the data in the study and takes responsibility for the integrity of the data and the accuracy of the data analysis.

Concept and design: Ong, Toth

Acquisition, analysis, or interpretation of data: Ong, Cummings, Vajzovic, Mruthyunjaya, Toth

Drafting of the manuscript: Ong

Critical revision of the manuscript for important intellectual content: Ong, Cummings, Vajzovic, Mruthyunjaya, Toth

Obtained funding: Ong, Toth

Study supervision: Toth

Additional Contributions:

Du Tran-Viet, BS, Vincent Tai, MS and Katrina Winter, BS provided assistance with image processing and analysis, and Sandra Stinnett, DrPH completed statistical analysis for this study.

Conflict of Interest Disclosures:

All authors have completed and submitted the ICMJE Form for Disclosure of Potential Conflicts of Interest and none were reported.

Results: Mean age (± SD) was 9.5 ± 5.5 years for the 28 children (and 29 eyes) with clinical imaging. A comparison between imaging modalities revealed OCT features that were not visible on photos or FA: exudates in multiple retinal layers (n=23); small pockets of subretinal fluid (n=4); outer retinal atrophy overlying fibrotic nodules (n=7); and small preretinal hyperreflective OCT dots (n=25). Next, a comparison with light micrographs helped relate OCT findings to pathological features: hyperreflective linear structures on OCT appeared consistent with cholesterol crystals, small hyper-reflective dots with macrophages, outer retinal tubulations with rosettes; and analogous OCT-histopathology features: intraretinal vessels entering fibrotic nodules, and retinal pigment epithelium excrescences under subretinal fluid. OCT analysis revealed intraretinal cystoid spaces in 19 eyes but in 9/19, this did not correlate with cystoid macular leakage, rather fluorescein leakage was observed from peripheral telangiectatic vessels. Additionally, exudates were intraretinal only (n=6) or both intraretinal and subretinal (n=17); none were subretinal only. In eyes with follow-up, new fibrosis developed in 8/17 eyes. Fibrosis developed in 5/5 eyes with baseline subretinal fluid versus 3/12 without (75% difference; 95% CI, 22%−92%) and in 7/9 eyes with subretinal exudates versus 1/8 without (65% difference; 95% CI, 16%−89%).

Conclusions and Relevance: OCT may show transient and permanent effects of Coats' disease on the retina. These results suggest that exudates and fluid in the macular subretinal space appear later in disease and may result in fibrosis formation. Further studies are needed to confirm if early treatment could prevent vision-threatening macular fibrosis.

SUMMARY STATEMENT

Clinical and histopathologic comparisons in Coats' disease yield new information on the intra and subretinal features of the disease.

Keywords

Coats' disease; Optical coherence tomography; OCT; SDOCT; handheld OCT; multimodal imaging; histopathology; pediatric retina; subretinal fibrosis; fibrotic nodule

INTRODUCTION

The advent of wide-field imaging including the use of wide-field fundus photography (FP) and fluorescein angiography (FA) under anesthesia has improved the visualization of peripheral vascular findings in Coats' disease.[1–3] Information about cross-sectional ultrastructural changes in Coats' disease, however, remains lacking in earlier stages of disease since histopathological specimens usually included eyes that were enucleated for advanced disease.[4–9] Microscopic examination of enucleated eyes have shown lipid laden macrophages and cholesterol clefts in the sensory retina and subretinal fluid (SRF).[4–9]

Optical coherence tomography (OCT) provides a unique opportunity for cross-sectional ultrastructural analysis of the retina in a live patient. Because the resolution of OCT is at the micrometer level, OCT findings are arguably comparable to histology. This provides clinicians with a powerful tool to examine Coats' disease, especially in earlier disease. However, publications on OCT findings in Coats' disease to date are limited to single case

reports and small case series[10–14] and there has yet to be a study that combines both OCT and histopathologic analysis. The objective of this study was therefore to compare the appearance of retinal and subretinal findings in Coats' disease on OCT with FP, FA and relevant histopathologic analysis. Using these findings, we also examined the pathogenesis of macular fibrosis, which causes irreversible vision loss in Coats' disease.[15]

METHODS

This was a retrospective cohort study of all patients under age 21 who were diagnosed with Coats' disease, presented before treatment to Duke Eye Center between 12/1/2002 to 1/31/2018 and were imaged with OCT, FP and FA. The study was conducted between 07/26/2017 to 04/29/2018, was designed in accordance with the tenets of the Declaration of Helsinki, was approved by the Institutional Review Board at Duke University and was Health Insurance Portability and Accountability Act compliant.

Diagnosis of Coats' disease included fulfilling clinical criteria of having idiopathic retinal telangectasia with or without exudation and/or exudative retinal detachments. Demographic information and staging of Coats' disease were documented. Affected eyes were divided based on clinical examination, FP or FA into five stages of disease as described by Shields et al.[16]

FP (color, red-free) and FA were obtained using tabletop systems: Zeiss FF450 (Carl Zeiss Meditec, Okerkochen, Germany), ultra-wide field on Optos 200Tx (Optos, Inc., Dunfermline, United Kingdom); or during examination under anesthesia (EUA): with RetCam 2 (Clarity Medical Systems, Pleasanton, CA). OCT was attained using tabletop time-domain or spectral-domain OCT (Stratus OCT [Carl Zeiss Meditec, Inc., Dublin, CA] or Spectralis HRA-OCT [Heidelberg Engineering, Heidelberg, Germany]) or portable handheld SD-OCT (Leica Microsystems, Research Triangle Park, NC).

Paraffin embedded tissue from four enucleated eyes were obtained from the Duke Biorepository and Precision Pathology Center. Using light microscopy, these histologic sections were examined and compared with in-vivo OCT findings.

Statistical analysis was performed using JMP Pro version 13.0 (SAS Institute Inc, Cary, NC). 95% confidence intervals (CI) for percent difference between groups were calculated and statistical significance was represented by 95% CI that do not contain 0.

RESULTS

Twenty-eight patients, and 29 eyes, met entry criteria; mean age (SD, range) at presentation was 9.5 (5.5, 1.1–18.7) years and 24 (86%) were male. Race was white (n=11); black (n=7); Asian (n=4); Hispanic (n=1) or unreported (n=5). At presentation, stages of disease were 1 (n=1), 2A (n=4), 2B (n=12), 3A1 (n=8), and 3A2 (n=4). Snellen or equivalent visual acuities was recorded at presentation for 26 eyes and ranged from 20/20 to 20/8000 (median 20/200).

Clinical information from four biorepository eyes was reviewed. 2 patients were male. These were younger patients [mean age was 1.3 (0.7, 0.4–1.9) years] with more severe disease:

enucleation was due to concern for retinoblastoma in three eyes with total retinal detachment, or uncontrolled glaucoma in one blind and painful eye. None of the enucleated eyes had received any vitreoretinal surgery. One eye was treated with laser cyclophotocoagulation one month before enucleation.

Baseline Imaging

Color or red-free photography was performed in clinic in 21/29 eyes (5 tabletop: age range 8.5–18.7 years, and 16 ultra-wide field: 4.0–18.4 years) and during EUA in 8/29 (1.1–14.5 years). FA, not performed in 4 eyes, was obtained in clinic in 13/25 eyes [3 tabletop (15.6–18.4 years); 10 ultra-wide field (8.2–18.7 years)] and during EUA in 12/25 (1.1–14.5 years). Twenty-five of 29 eyes underwent OCT in clinic (6 time-domain and 19 spectral-domain; 4.0–18.7 years) while 4/29 had OCT with a hand-held device during EUA (spectral-domain; 1.1–4.4 years).

Clinical and Histopathologic Findings

Exudates (Figures 1-2, eFigure 1 in the Supplement)—Twenty-eight of 29 eyes had exudates on photographs; 23 within the macula and 20 within the fovea. On OCT, the exudates appeared as bright hyperreflective foci or broad sheets and were observed in the following retinal layers: nerve fiber, NFL (n=7), ganglion cell, GCL (n=8), inner plexiform, IPL (n=15), inner nuclear, INL (n=19), outer plexiform, OPL (n=19), outer nuclear, ONL (n=23), and in the subretinal space (n=17). Two eyes had highly hyperreflective linear structures (within subretinal exudates and SRF respectively) on OCT corresponding to refractile cholesterol crystals on photographs. On light micrographs, eosinophilic exudates were also observed in every retinal layer and subretinally, and cholesterol clefts were seen in the SRF.

On OCT, the highest density of exudates were observed in the upper half of the ONL (correlate for histological Henle fiber layer, HFL, which is part of OPL[17]) in 13 eyes (9 of these were star shaped on photographs), and in the subretinal space in 10 eyes. While exudates were found intraretinally only in 6 eyes, exudates were observed both intraretinally and subretinally in 17 eyes. Notably, no eye had subretinal exudates in the absence of intraretinal exudates.

Retinal Detachment (Figure 2)

Retinal detachment was apparent on photos in 12 eyes, and involved the macula and foveal center in 6 and 4 eyes respectively. OCT also demonstrated macular SRF in these 6 eyes. In an additional 4 eyes, OCT illustrated a small pocket of macular SRF that was not visible on photographs (Figure 1B inset). OCT further showed small hyper-reflective dots in the SRF and retina in 3/10 eyes. Importantly, the small hyper-reflective dots were observed in areas devoid of exudates on photographs and en-face infrared images. On light micrographs, the retina surrounding SRF was thickened and diffusely infiltrated by macrophages.

Light micrographs also illustrated cholesterol crystals and macrophages in the eosinophilic SRF, and retinal pigment epithelium (RPE) excrescences with RPE thinning underlying SRF. On OCT, these RPE excrescences were not well defined due to shadowing from exudates but

in two eyes, a few hyperreflective RPE excrescences were seen under SRF in areas devoid of exudates.

Fibrosis (Figures 3-4, eFigure 2 in the Supplement)—Seven of 29 eyes presented with macular fibrosis. On photographs, the fibrosis appeared foveal-involving, nodular, pigmented, and surrounded by dense exudation. OCT also showed that macular fibrosis was nodular, intermediately hyperreflective with areas of intense hyperreflectivitiy due to pigment, and surrounded by intraretinal and subretinal exudates. OCT further showed the presence of hyporeflective cystoid spaces [in the GCL (n=3), INL (n=7) and ONL (n=3)] and overlying outer retinal atrophy in 7/7 eyes. In 3 of these 7 eyes, the hyperreflective material associated with the fibrotic nodule transversed through all layers of the retina and created a full-thickness macular hole. On light micrographs, the outer retina overlying all fibrotic nodules were also observed to be atrophic.

On histologic sectioning, four and one fibrotic nodules were observed in two eyes respectively. All fibrotic nodules contained cholesterol clefts intermixed with macrophages, pigment granules, and fibrinous material. Multinucleated giant cells, lymphocytes, plasma cells and capillaries were also observed. One of these nodules also had a fibrous capsule and two nodules were accompanied by rosette formation in the overlying retina. Eyes with fibrotic nodules on OCT were examined and 3/7 eyes had a corresponding hyperreflective tubule with a hyporeflective core in the overlying and surrounding retina. One eye without fibrosis but with extensive macular atrophy was also observed to have these tubular structures on OCT (eFigure 3 in the Supplement).

Photographs demonstrated a prominent retinal vessel that appeared to dive towards the nodule in 6 of 7 eyes, and this was accompanied by a few spots of hemorrhage in 1 eye. FA, available for 6 eyes with macular fibrosis, showed staining with areas of leakage (n=3), staining (n=2) or diffuse macular leakage (n=1). On OCT, a hyperreflective elongated structure with posterior shadowing, which was continuous with inner retinal vasculature and travelled toward the nodule, was observed in 4/7 eyes. On histologic sectioning, we observed a vessel from the inner retina approaching a fibrotic nodule found in the macula. Due to histologic processing, the neurosensory retinas were artificially detached from the RPE and choroid. All five fibrotic nodules were observed attached to the undersurface of and partially encircled by the neurosensory retina without any connection to the RPE/choroid. No nodule was accompanied by hemorrhage under the distant RPE or a break in the Bruch membrane.

Additional Clinical Findings

OCT showed small preretinal hyperreflective OCT dots in 25 eyes, epiretinal membrane in 11 eyes and inner surface wrinkling in 12 eyes (Figure 2B). OCT further demonstrated intraretinal hyporeflective cystoid spaces in 19 eyes. Seven of these eyes had coexisting macular fibrosis. One eye had coexisting macular atrophy without fibrosis; the cystoid spaces were observed in the INL, and FA demonstrated a window defect (eFigure 3 in the Supplement). Of the remaining eleven eyes, two demonstrated cystoid macular leakage on FA with intraretinal fluid observed in the INL and ONL (eFigure 4 in the Supplement); while nine had no macular hyperfluorescence on FA, but had intraretinal cystoid spaces

between peripheral leaking aneurysms and the fovea, and cross-sectionally in the GCL (n=1), INL (n=7) and ONL (n=9).

Evolution of Clinical Findings After Treatment

19 eyes had ≥ 6-month follow-up after treatment (average 41 ± 42 months). Seven of these eyes had laser and/or cryopexy, 9 had this treatment plus anti-vascular endothelial growth factor (VEGF) injections, 2 had vitreoretinal surgery and 1 had vitreoretinal surgery with anti-VEGF injections.

Macular exudates and SRF improved or resolved after treatment in all 14/14 eyes with macular exudates and 5/5 eyes with macular SRF at baseline. No eye developed new macular exudates or SRF. In comparison, of the 17 eyes with no macular fibrosis at baseline, 8 developed new macular fibrosis (6 were fovea-involving). Of the 16 eyes with no previous macular atrophy, 9 developed new macular atrophy (5 were foveal-involving). No eye had resolution of macular fibrosis or atrophy.

The likelihood of developing new macular fibrosis at the final follow-up was 75% higher when macular SRF was present (5/5 eyes) versus absent (3/12 eyes) (95% CI, 22%−92%); and 65% higher when macular subretinal exudates were present (7/9 eyes) versus absent (1/8 eyes) (95% CI, 16%−89%) on OCT at baseline. Moreover, the development of macular atrophy was associated with the development of macular fibrosis: the proportion of eyes that developed macular atrophy was 63% higher in eyes that developed macular fibrosis (7/8) versus those with no new macular fibrosis (2/8) (95% CI, 12%−88%). eFigure 5 in the Supplement illustrates an eye that developed macular and extramacular fibrosis post-treatment.

DISCUSSION

To our knowledge, this is the first study of pediatric Coats' disease to compare OCT with FP, FA and relevant light micrographs. A literature search on PubMed using the terms "optical coherence tomography", "Coats' disease", "histology", "pathology" between January 1, 2007 and April 29, 2018 revealed no prior published manuscripts on this topic. Of note, imaging in clinic was possible in children as young as age four with ultra-wide-field retinal imaging and OCT. This may have been, in part, because both systems lack white light illumination that can be bothersome to young children.

This study showed multiple advantages in adding OCT to traditional imaging with photography and FA in Coats' disease. First, OCT documented exudates in all retinal layers, which could not be appreciated on photographs. Second, OCT explained the macular star pattern of exudation in some eyes with Coats' disease. These exudates for the most part accumulated in the upper half of the ONL; previous reports had shown that HFL corresponds to the usually hyporeflective ONL.[17] Third, while photographs showed macular detachment in six eyes, OCT demonstrated SRF in ten eyes. Subtle SRF may be missed on clinical exam or with non-OCT based imaging. Fourth, OCT demonstrated the presence of extensive outer retinal atrophy above fibrotic nodules, which is not appreciated on photographs. Fifth, OCT is the only clinical imaging modality capable of showing small

preretinal hyperreflective OCT dots, which may represent lipid, inflammatory cells or red blood cells.

Furthermore, this study revealed several observations on OCT that may be related to features on histopathologic analysis. Cholesterol clefts and macrophages are hallmark features of Coats' disease and were observed in the enucleated specimens. Hyperreflective linear structures resembling cholesterol crystals were also observed in two eyes on OCT, both on the cross-sectional image and en-face infrared image. Additionally, small hyper-reflective dots were observed in 3/10 eyes with SRF in areas devoid of exudates, and we speculate that they represent the macrophages observed on light micrographs. These hyper-reflective subretinal and intraretinal dots have been previously observed in central serous chorioretinopathy, and were theorized to represent macrophages.[18] Light micrographs showed macrophages within exudates as well but these would be difficult to identify on OCT since exudates are also hyper-reflective.

Other findings found on both light microscopy and OCT include RPE excrescences under SRF, retinal rosettes, and intraretinal vessels approaching a fibrotic nodule. RPE excrescences were observed under extensive SRF in two eyes on both light micrographs and OCT. On light micrographs, retinal rosettes overlying two fibrotic nodules were observed. A corresponding hyperreflective tubule in the outer retina was also observed on OCT in 3/7 eyes with fibrotic nodules and 1/1 eye without fibrosis but with extensive atrophy. These tubules have a hyperreflective wall surrounding a hyporeflective core and resemble "outer retinal tubulations" previously described in macular degeneration, Bietti's crystalline dystrophy and choroidemia.[19] The appearance of outer retinal tubulations has been proposed to be due to degenerating photoreceptors becoming arranged in a tubular fashion,[19] while rosettes in Coats' disease are postulated to represent secondary changes due to retinal degeneration or detachment.[20] We are the first to describe outer retinal tubulations on OCT in Coats' disease and suspect that the rosettes previously described in Coats' disease represent outer retinal tubulations since both are lined by an external limiting membrane with photoreceptor segments either lining the wall or projecting into the lumen.[20, 21]

An intraretinal vessel approaching a fibrotic nodule was observed on light micrographs in one biorepository eye. On OCT, corresponding hyperreflective elongated structures from the inner retinal vasculature entering the nodules were observed in 4/7 eyes. Additional findings of retinal vessels diving down into the lesion (6/7 eyes) with adjacent dots of blood (1/7 eye) on photographs, leakage (4/6 eyes) on FA, and cystoid intraretinal spaces (7/7 eyes) on OCT possibly due to leakage from neovascularization (versus atrophy) all lend support to the hypothesis that type 3 neovascularization can occur in fibrotic nodules. This study therefore supports existing literature that reported the presence of neovascularization in fibrotic nodules in Coats' disease.[22, 23] However, we did not observe any hemorrhage under RPE or Bruch membrane disruption that would suggest a connection between the subretinal nodule with the choroid. Chang and colleagues analyzed 13 eyes with macular fibrous nodules and similarly did not observe hemorrhage below RPE,[5] but others had observed that Bruch membrane can be disrupted with blood vessels extending from the choroid to the bottom of a fibrotic mound.[20, 24]

Consistent with prior reports, we showed that exudative fluid and material may diffuse posteriorly to the macula, and from the intraretinal tissue to the subretinal space.[24, 25] This is supported by findings of cystoid spaces without leakage between extramacular lesions and the fovea, and absent on the other side of the fovea. Furthermore, while some eyes only have intraretinal exudates, all eyes with subretinal exudates also have intraretinal exudates. These findings suggest that fluid or exudates in the macular subretinal space are seen later in disease.

We also found that fluid or exudates in the macular subretinal space were associated with new macular fibrosis formation. Subretinal exudates have previously been postulated to incite the recruitment of phagocytic inflammatory cells that lead to fibrosis.[26, 27] Manschot and De Bruijn demonstrated on electron microscopy that phagocytic cells in an eye with Coats' disease and subretinal fibrosis had empty lipid vacuoles and 1) pigment granules within vacuoles, or 2) native pigment granules embedded directly in cytoplasm. They also observed 1) pigment epithelium cells that had taken on a fiber producing ability and 2) typical fibroblasts.[26] Since native pigment granules embedded in cytoplasm are found in RPE cells while pigment granules in vacuoles are found in macrophages, the authors concluded that subretinal exudates cause the recruitment of RPE cells that differentiate into phagocytic cells with the ability to produce fiber, as well as macrophages and fibroblasts that migrate from the retina. We similarly observed on light micrographs the presence of macrophages and multinucleated giant cells in fibrotic nodules. However, without electron microscopy, we could not determine if pigment granules were in vacuoles or embedded in the cytoplasm. Using light micrographs, we further observed the presence of an intraretinal vessel approaching the fibrotic nodule, and proliferating capillaries within the nodule. Therefore, the inflammatory cascade that causes fibrosis in Coats' disease may also recruit endothelial cells which proliferate and form new blood vessels.

Limitations of this study include its retrospective nature, non-standardized imaging and small sample size, which restricts the power to detect differences between subgroups. The comparison between OCT findings and histopathology was also limited given the more severe disease seen in enucleated eyes.

Conclusions

Fluid and exudates appear in the macular subretinal space later in disease and are associated with new macular fibrosis. We therefore postulate that early treatment before exudation into the macular subretinal space may prevent macular fibrosis, although this cross-sectional study cannot confirm this relationship. This study also highlights the importance of OCT in multimodal imaging. OCT augments photographs and FA, and demonstrates features that are comparable to histopathologic findings.

Supplementary Material

Refer to Web version on PubMed Central for supplementary material.

Acknowledgments

Funding/Support:

This publication was supported by The International Retinal Research Foundation; The Hartwell Foundation; The Andrew Family Charitable Foundation; NIH Grants: 1RO1 EY025009; P30 EY005722; and UL1 RR024128 (Pilot project grant) from Duke Translational Research Institute and NIH Roadmap for Medical Research. Its contents are solely the responsibility of the authors and do not necessarily represent the official view of NIH.

Role of the Funder/Sponsor:

The sponsors or funding organizations had no role in the design or conduct of this research; collection, management, analysis and interpretation of the data; preparation, review or approval of the manuscript; and decision to submit the manuscript for publication.

References

1. Blair MP, Ulrich JN, Elizabeth Hartnett M, Shapiro MJ. Peripheral retinal nonperfusion in fellow eyes in coats disease. Retina. 9 2013;33(8):1694–1699. [PubMed: 23974953]
2. Shane TS, Berrocal AM, Hess DJ. Bilateral fluorescein angiographic findings in unilateral Coats' disease. Ophthalmic Surg Lasers Imaging. 2011;42 Online:e15–17. [PubMed: 21323189]
3. Suzani M, Moore AT. Intraoperative fluorescein angiography-guided treatment in children with early Coats' disease. Ophthalmology. 6 2015;122(6):1195–1202. [PubMed: 25824326]
4. Mandava N, Yannuzzi LA. Coats disease. Philadelphia: WB Saunders; 1999.
5. Chang MM, McLean IW, Merritt JC. Coats' disease: a study of 62 histologically confirmed cases. J Pediatr Ophthalmol Strabismus. Sep-Oct 1984;21(5):163–168. [PubMed: 6502405]
6. Farkas TG, Potts AM, Boone C. Some pathologic and biochemical aspects of Coats disease. Am J Ophthal. 1973;79:289–304.
7. Theodossiadis GP. Some clinical, fluorescein-angiographic and therapeutic aspects of Coats disease. J Pediatr Ophthalmol Strabismus. 1974;16:257–262.
8. Eagle RC. Coats disease. Philadelphia: WB Saunders; 1999.
9. Haller JA. Coats disease. Vol 2 2nd ed St Louis: CV Mosby; 1994.
10. Shields CL, Mashayekhi A, Luo CK, Materin MA, Shields JA. Optical coherence tomography in children: analysis of 44 eyes with intraocular tumors and simulating conditions. J Pediatr Ophthalmol Strabismus. Nov-Dec 2004;41(6):338–344. [PubMed: 15609518]
11. Henry CR, Berrocal AM, Hess DJ, Murray TG. Intraoperative spectral-domain optical coherence tomography in Coats' patients. Ophthalmic Surg Lasers Imaging Retina. 2012;43:e80–e84.
12. Kessner R, Barak A, Neudorfer M. Intraretinal Exudates in Coats' Disease as Demonstrated by Spectral-Domain OCT. Case Rep Ophthalmol. 1 2012;3(1):11–15. [PubMed: 22615695]
13. Hautz W, Golebiewska J, Kocyla-Karczmarewicz B. Optical Coherence Tomography and Optical Coherence Tomography Angiography in Monitoring Coats' Disease. J Ophthalmol. 2017;2017:7849243. [PubMed: 28377823]
14. Rabiolo A, Marchese A, Sacconi R, et al. Refining Coats' disease by ultra-widefield imaging and optical coherence tomography angiography. Graefes Arch Clin Exp Ophthalmol. 9 05 2017.
15. Ong SS, Buckley EG, McCuen BW 2nd, et al. Comparison of Visual Outcomes in Coats' Disease: A 20-Year Experience. Ophthalmology. 9 2017;124(9):1368–1376. [PubMed: 28461016]
16. Shields JA, Shields CL, Honavar SG, Demirci H, Cater J. Classification and management of Coats disease: the 2000 Proctor Lecture. Am J Ophthalmol. 5 2001;131(5):572–583. [PubMed: 11336931]
17. Lujan BJ, Roorda A, Knighton RW, Carroll J. Revealing Henle's Fiber Layer Using Spectral Domain Optical Coherence Tomography. Investigative Ophthalmology & Visual Science. 3 2011;52(3):1486–1492. [PubMed: 21071737]
18. Spaide RF, Klancnik JM Jr., Fundus autofluorescence and central serous chorioretinopathy. Ophthalmology 5 2005;112(5):825–833. [PubMed: 15878062]

19. Zweifel SA, Engelbert M, Laud K, Margolis R, Spaide RF, Freund KB. Outer retinal tubulation: a novel optical coherence tomography finding. Arch Ophthalmol 12 2009;127(12):1596–1602. [PubMed: 20008714]

20. Egerer I, Rodrigues MM, Tasman WS. Retinal Dysplasia in Coats Disease. Canadian Journal of Ophthalmology-Journal Canadien D Ophtalmologie. 1975;10(1):79–85. [PubMed: 1122421]

21. Litts KM, Messinger JD, Dellatorre K, Yannuzzi LA, Freund KB, Curcio CA. Clinicopathological correlation of outer retinal tubulation in age-related macular degeneration. JAMA Ophthalmol 5 2015;133(5):609–612. [PubMed: 25742505]

22. Sigler EJ, Calzada JI. Retinal angiomatous proliferation with chorioretinal anastomosis in childhood Coats disease: a reappraisal of macular fibrosis using multimodal imaging. Retina. 3 2015;35(3):537–546. [PubMed: 25170864]

23. Jumper JM, Pomerleau D, McDonald HR, Johnson RN, Fu AD, Cunningham ET Jr,. Macular fibrosis in Coats disease. Retina. 4 2010;30(4 Suppl):S9–14. [PubMed: 20419849]

24. Wise GN, Wangvivat Y. The exaggerated macular response to retinal disease. Am J Ophthalmol. 5 1966;61(5 Pt 2):1359–1363. [PubMed: 5938021]

25. Otani T, Yamaguchi Y, Kishi S. Serous macular detachment secondary to distant retinal vascular disorders. Retina. 10 2004;24(5):758–762. [PubMed: 15492631]

26. Manschot WA, De Bruijn WC. Coats' disease: Definition and pathogenesis. Br J Ophthal. 1967;51:145–157. [PubMed: 6019808]

27. Leber T Graefe-Saemisch-Hess Handbuch der gesamten Augenheilkunde. 2nd ed, band 7, teil 2, kap XA, II halfte. Engelmann, Leipzig; 1916:1267.

KEY POINTS

Question:

How is optical coherence tomography (OCT) useful in the assessment of Coats' disease?

Findings:

In 29 eyes from 28 children with Coats' disease, OCT analysis revealed axial location of fluid, exudates and atrophy, which were not visible with photographs and fluorescein angiograms. Distinct OCT morphologies, when compared to histologic findings from biorepository eyes with Coats' disease, were consistent with retinal anatomic changes, and intra- and subretinal cells and depositions.

Meaning:

OCT augments photographs and angiography to reveal transient and permanent effects of disease on the retina. These may be useful in monitoring disease activity and response to therapy.

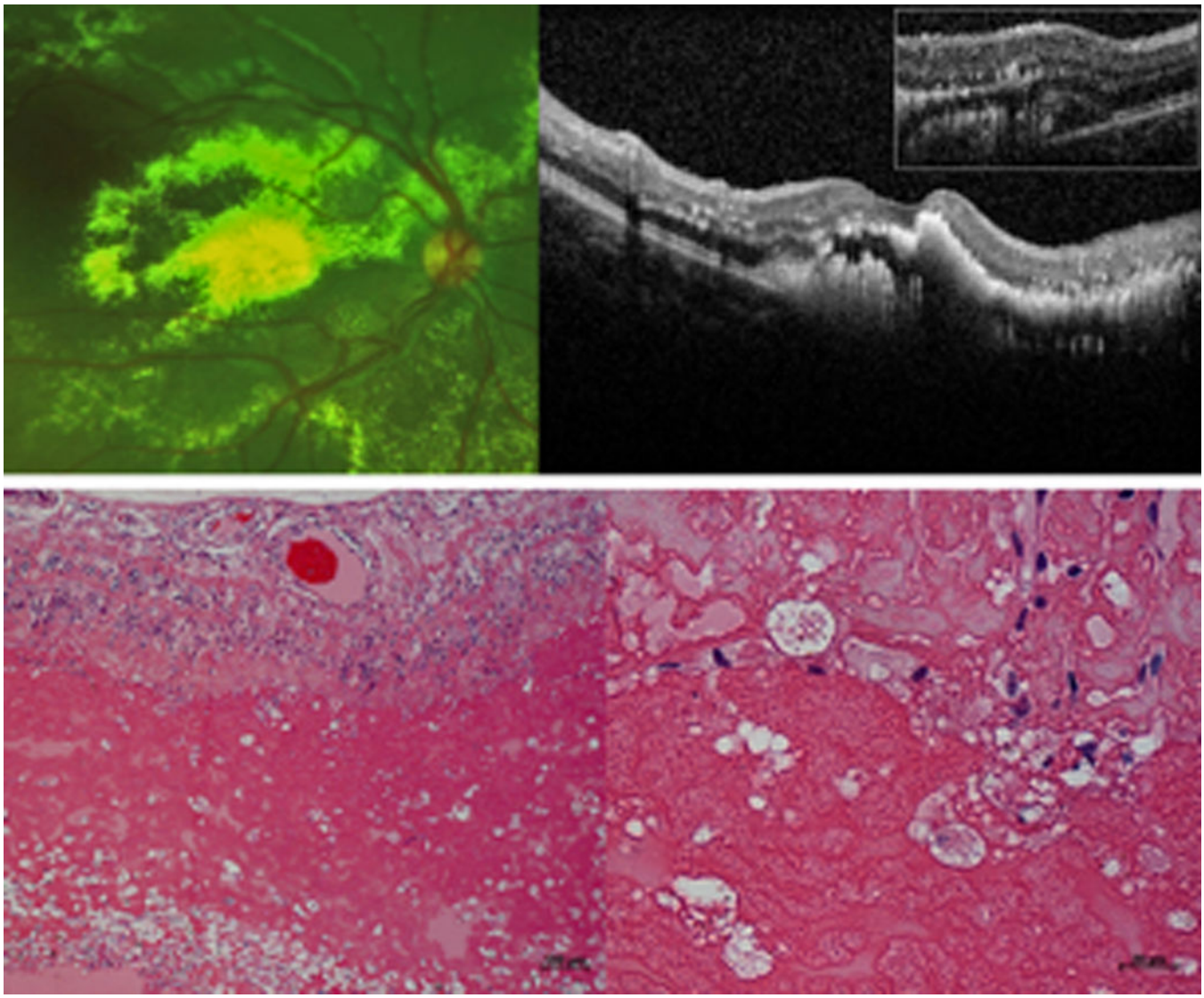

Figure 1. Exudates in Coats' disease on (A) fundus photograph and (B) optical coherence tomography, OCT from a 7-year-old boy, and (C) low power and (D) high power histopathologic staining with hematoxylin and eosin (H&E) from an enucleated repository eye.

The vertical and horizontal white dotted lines on the photograph correspond to the main and inset OCT line scans respectively, while the black dotted box on the low-power micrograph denotes the area shown in the high-power micrograph. OCT shows that exudates are found both intraretinally (yellow arrows) and subretinally (yellow arrowhead). The inset OCT demonstrates the presence of a subretinal fluid pocket (blue arrow) that is difficult to visualize on a 2-dimensional photograph. On light micrographs, exudates appear as pinkish eosinophilic material in multiple intraretinal layers and subretinally (yellow arrows). The subretinal exudates are interspersed in subretinal fluid (blue arrows). Higher power magnification demonstrates the presence of pigment and lipid laden macrophages (black arrows) amongst exudates (yellow arrow) in the subretinal space.

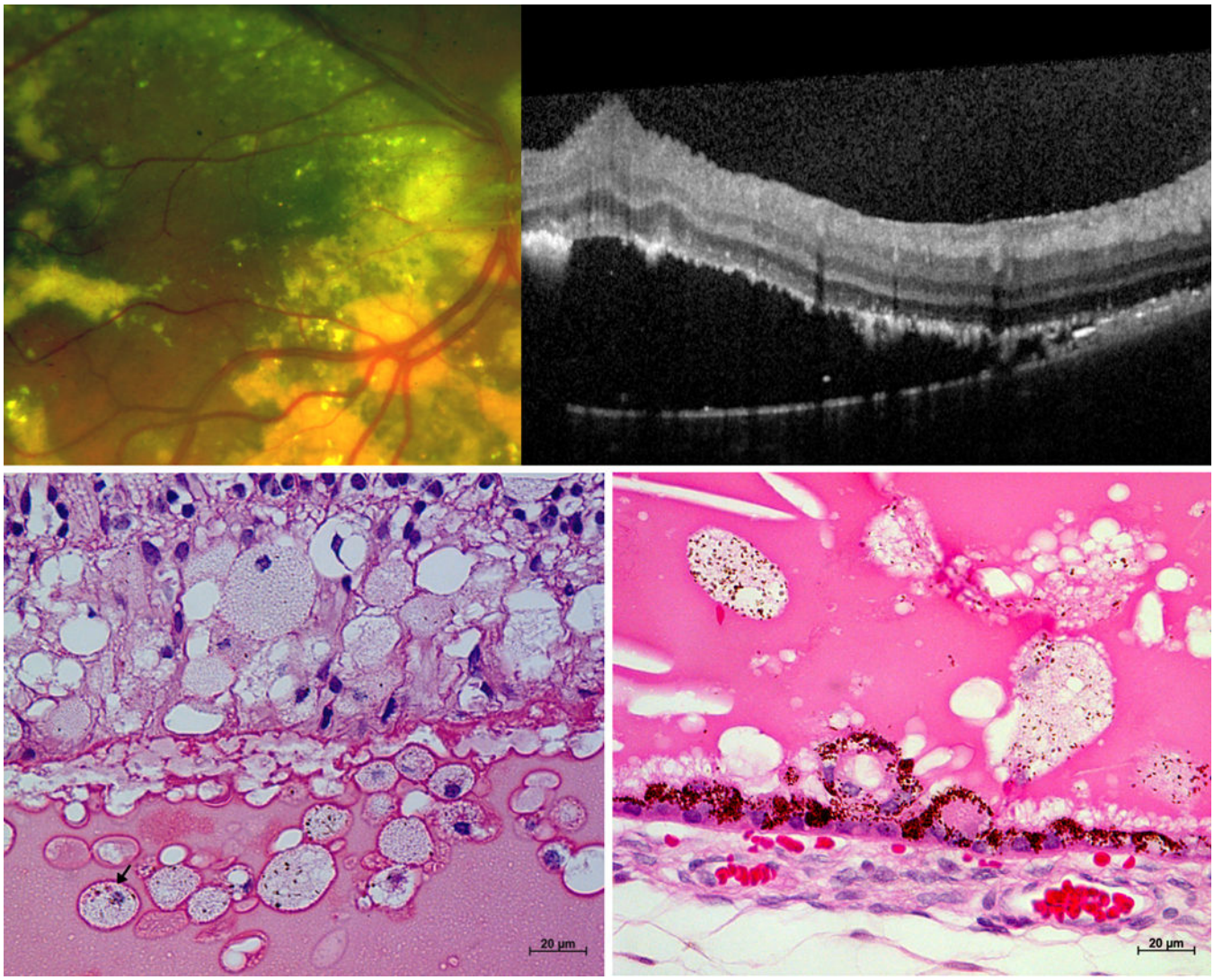

Figure 2. Retinal detachment in Coats' disease on (A) fundus photograph and (B) optical coherence tomography, OCT from a 17-year-old male, and (C-D) light micrographs from two enucleated biorepository eyes.

The horizontal white dotted line on the photograph corresponds to the OCT line scan. Subretinal fluid (blue arrow), exudates (yellow arrows), inner retinal wrinkling (white arrowhead), small preretinal hyperreflective OCT dots (orange arrows) and epiretinal membrane (pink arrow) are observed on OCT. Comparison of OCT and light micrographs demonstrate corresponding structures including hyperreflective linear cholesterol crystals (yellow arrowheads), retinal pigment epithelium excrescence (green arrows) and small intraretinal and subretinal hyperreflective dots in areas devoid of exudates (white arrows) that may correspond to macrophages (black arrows).

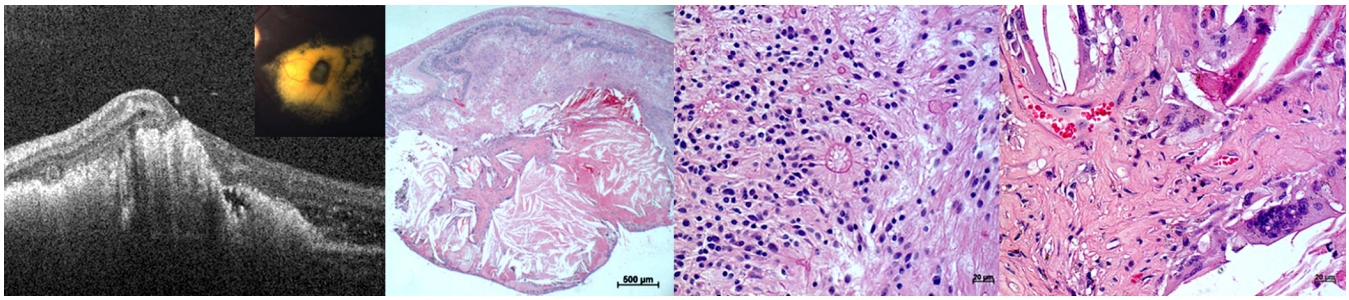

Figure 3. Fibrotic nodules in Coats' disease on (A) optical coherence tomography, OCT from a 4-year-old-boy, and (B) low and (C-D) high power light micrographs from an enucleated biorepository eye.

The horizontal white dotted line in the inset photograph corresponds to the OCT line scan while the black dotted boxes on the low power micrograph denote the areas above and within the cholesterol granuloma shown in the high-power micrographs. A hyperreflective tubule with a hyporeflective core (green arrow) overlying exudates (yellow arrow) and a fibrotic nodule (red arrows) with subretinal fluid (blue arrow) is observed on OCT. These appear to correspond to intraretinal rosettes (green arrows) in disorganized retina overlying the cholesterol granuloma on high power light micrograph. Other notable findings on light micrograph include a fibrous capsule surrounding the cholesterol granuloma (black arrowheads), as well as multinucleated giant cells with pigment granules (black arrows) surrounding cholesterol clefts (yellow arrowheads), proliferating capillaries (red arrowheads) and fibrinous material (red arrows) within the cholesterol granuloma.

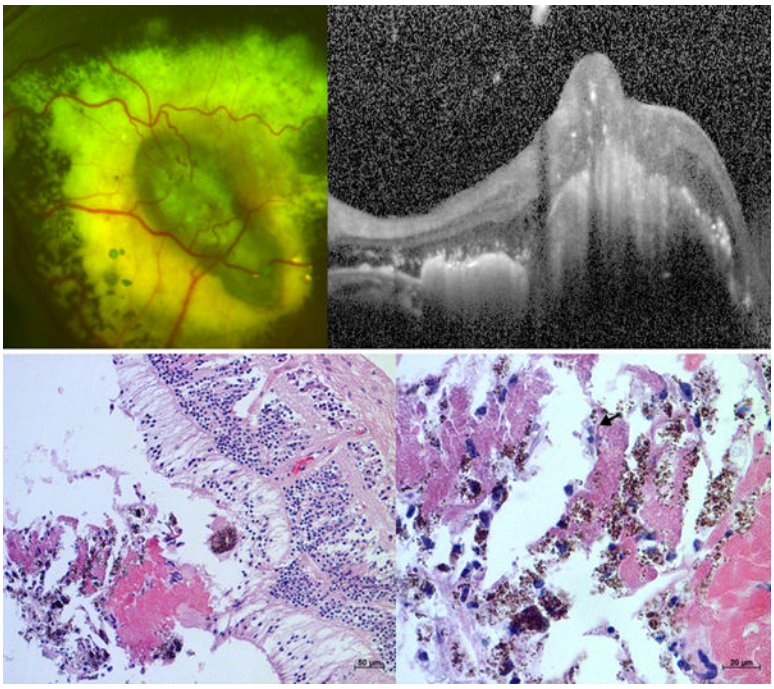

Figure 4. Fibrotic nodules in Coats' disease on (A) fundus photograph and (B) optical coherence tomography, OCT from an 8-year-old boy, and (C) low and (D) high power light micrographs from an enucleated biorepository eye.

The horizontal white dotted line on the photograph corresponds to the OCT line scan while the black dotted box on the low power micrograph denotes the area shown in the high power micrograph. Retinal vessels diving into the lesion (white arrows) are observed on fundus photograph, light micrograph and possibly OCT. Other notable findings include an adjacent dot of blood (white arrowhead) on photograph; atrophy of the outer retinal layers above the nodule (red arrows) and adjacent subretinal exudates (yellow arrow) on OCT; and multinucleated giant cells (black arrows) surrounding cholesterol clefts (yellow arrowheads) with deposition of fibrinous material (red arrows) on light micrographs.

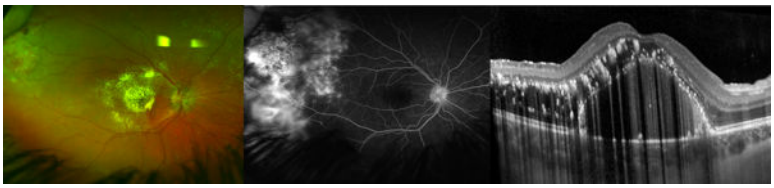

Figure 5. Macular intraretinal cystoid spaces in Coats' disease that do not correspond to angiographic leakage as demonstrated on fundus photograph (A), fluorescein angiography, FA (B) and optical coherence tomography, OCT (C) from an 11-year-old-boy.

The horizontal white dotted line on the photograph corresponds to the OCT line scan. There is no fluorescein leakage in the macula. On OCT, there are cystoid intraretinal spaces (blue arrow), subretinal fluid (blue arrowhead), and exudates (yellow arrow) in multiple retinal layers. A comparison with FA shows that the intraretinal cystoid spaces, subretinal fluid and exudates observed on OCT are mostly located between the fovea (white arrowhead) and peripheral telangiectatic vessels that leak (white arrow).